Organized Multi-Km Surface Stress Convergence Lines in Tropical Cyclone Surface Wind Retrievals

Ralph Foster[1]
With important contributions from
Jerome Patoux[2], Chris Wackerman[3], Jochen Horstmann[4],
Hans Graber[5], Mike Caruso[5]
[1]Applied Physics Laboratory, U of WA; [2]Atmospheric Sciences, U of WA;
[3]General Dynamics; [4]NATO Undersea Research Center; [5]RSMAS, U of Miami

RESEARCH SUPPORTED BY: ONR PHYSICAL OCEANOGRAPHY & MARINE METEOROLOGY;
NASA IOVWST. RADARSAT-1 IMAGERY ACQUIRED THROUGH HURRICANE WATCH AO

Multi-km-Scale Surface Wind Conv./Div. Patterns

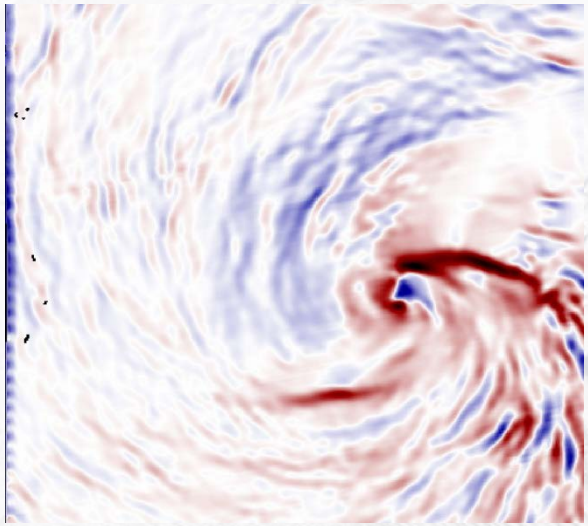

Malakas 22

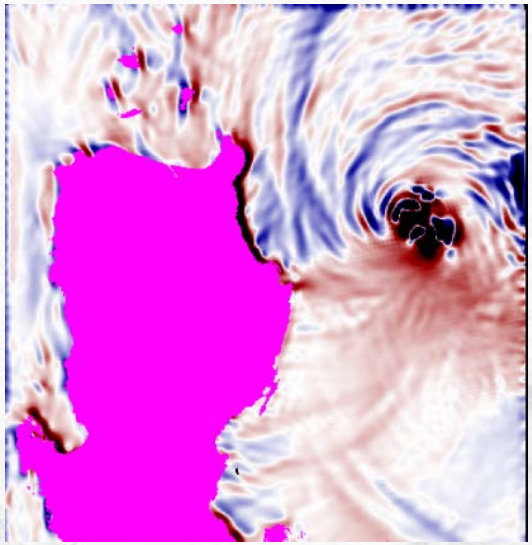

Megi 17

Ike

Red: Conv.
Blue: Div.

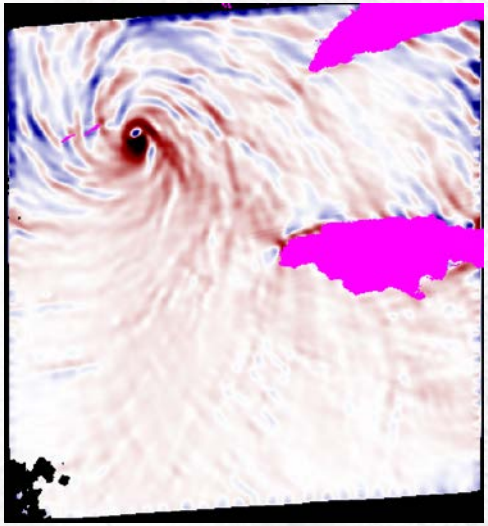

Lili

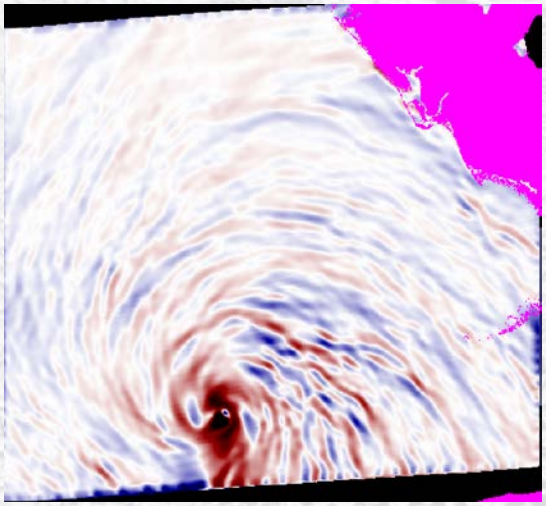

Katrina 27

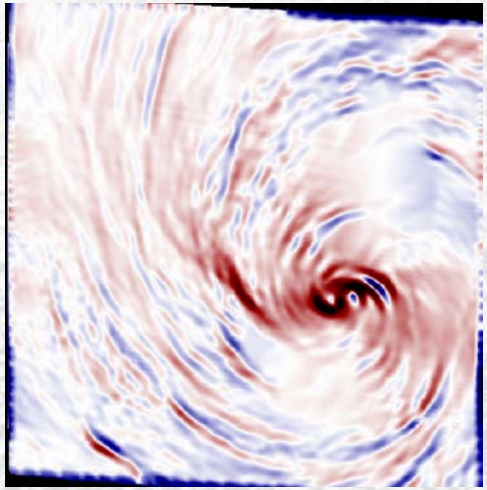

Helene 20

SLP-Filtered Tropical Cyclone (TC) SAR Wind Vector Fields (see Poster 23)

- SLP acts as a low-pass filter
  - Forces dynamical consistency
  - Winds at 1 km pixels
- Can calculate (hopefully) credible derivative fields
- **Consistent signature in all SAR TC divergence fields**:
  - *O*(~10 km) wavelength (λ) convergence bands
  - h (~ 1 km) is PBL depth
  - Look like PBL rolls, but aspect ratio (λ/h) is too large
- *O*(1-3 km) PBL rolls are very common feature of TC PBL

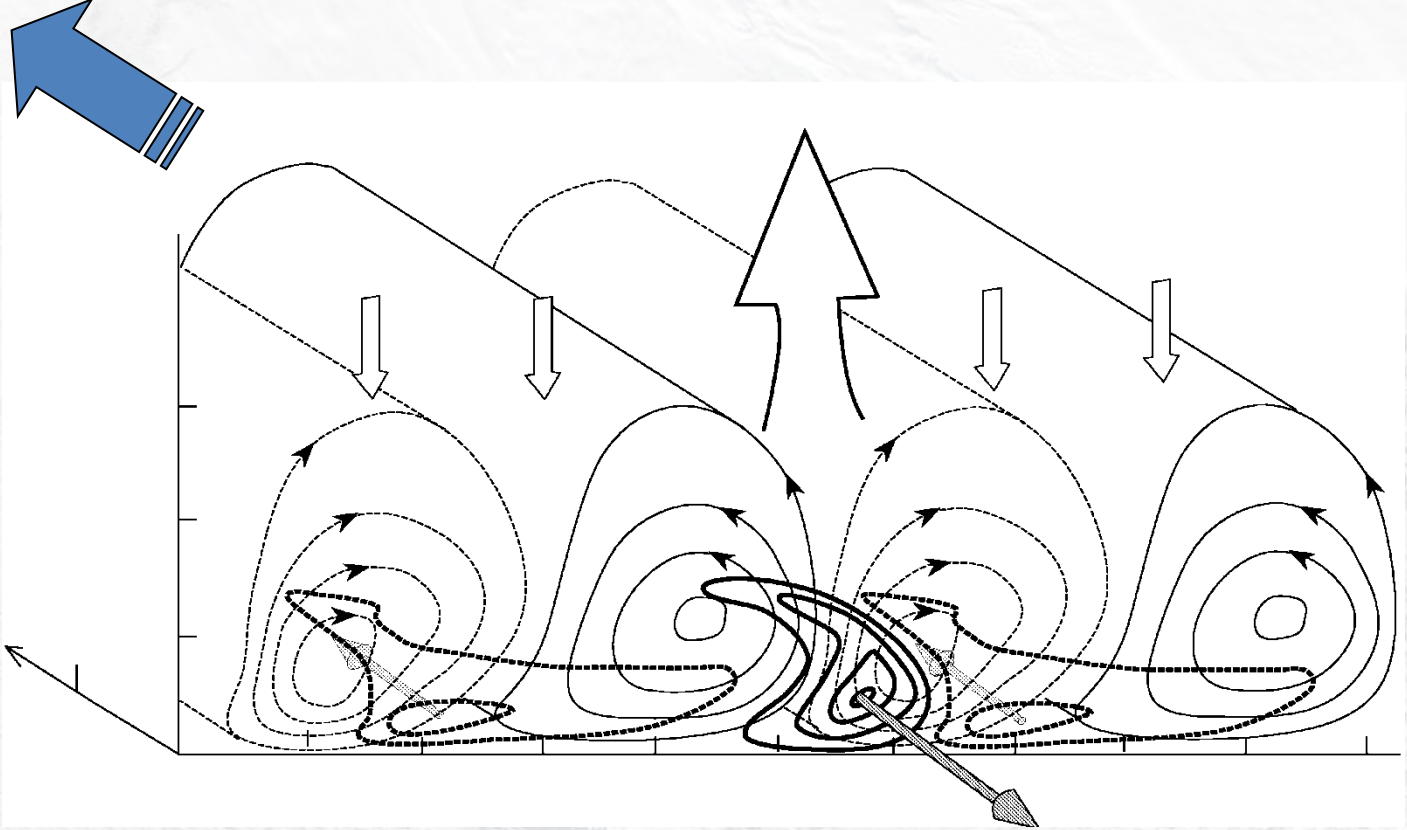

Wavelength: Larger-scale structures ~ 1500 to 2000 m
Smaller-scale structures ~ 300 to 700 m

Velocity Perturbations: +/- 7 m s^{-1} typical
up to +/- "10s of" m s^{-1} small-scale

Orientation: Typically along-mean TCBL wind, wide variability

Prevalence: Roll-scale structures common, (35% to 70%)
Streak-scale structures: ***Most likely usually present***

Science Hypothesis

- **THE CONVERGENCE LINES ARE THE SIGNATURE OF LARGE ASPECT RATIO TC PBL ROLL VORTICES**
  - Theory and observations agree that the common TC PBL rolls have aspect ratio *O*(2-4)
  - Large aspect ratio rolls are weak; not expected to survive competition with much faster-growing dominant rolls.
- Proposed Mechanism: **UPSCALE ENERGY TRANSFER FROM DOMINANT ($\lambda \sim$ 1-3 KM) MODES INTO WEAK ($\lambda \sim$ 10 KM) MODES THROUGH LOW-ORDER *RESONANT TRIAD WAVE-WAVE* INTERACTION**
  - Based on 2-D Ekman layer model of Mourad and Brown (1990);
  - +6 contributions omitted in MB90

Single-Wave Roll Theory
Nonlinear Stability

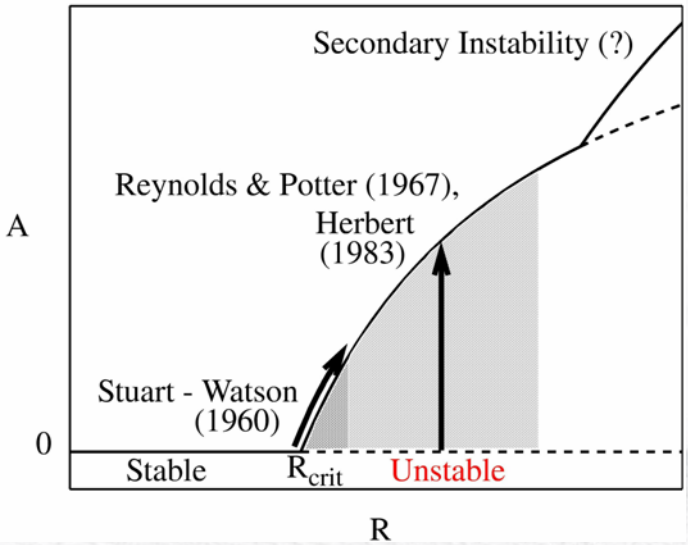

$$\lambda = a + i\omega = \frac{1}{A}\frac{dA}{dt} + i\frac{d\eta}{dt} = \lambda_0 + A^2\lambda_1 + A^4\lambda_2 + \cdots$$

$$\underset{\sim}{q} = 2real\left[\sum_{n=0}^{\infty} A^n e^{in(\alpha x - \omega t)} \sum_{m=0}^{\infty} A^{2m} \underset{\sim}{q}_{nm}(z)\right]$$

- "Stretch" eigenvalue, λ_0, in powers of nonlinear amplitude, *A(t)*.
- Expand eigenfunction, q_{10}, in harmonics of fundamental wavenumber, α, and forced modifications
  - Forced fundamental modifications are orthogonal to linear mode
  - Determine Landau Coefficients (the λ_i)
- Estimate equilibrium Amplitude (*dA/dt* = 0) & structure, ***q***

Standard Single-Wave PBL Roll Model

Table 5.1 Contributions to the nonlinear perturbation up to the fifth Landau Coefficient

Order	Landau	q_0	q_1	q_2	q_3	q_4	q_5	q_6	q_7	q_8	q_9	q_{10}	q_{11}
1		MF											
A	λ_0		q_{10}										
A^2		q_{01}		q_{20}									
A^3	λ_1		q_{11}		q_{30}								
A^4		q_{02}		q_{21}		q_{40}							
A^5	λ_2		q_{12}		q_{31}		q_{50}						
A^6		q_{03}		q_{22}		q_{41}		q_{60}					
A^7	λ_3		q_{13}		q_{32}		q_{51}		q_{70}				
A^8		q_{04}		q_{23}		q_{42}		q_{61}		q_{80}			
A^9	λ_4		q_{14}		q_{33}		q_{52}		q_{71}		q_{90}		
A^{10}		q_{05}		q_{24}		q_{43}		q_{62}		q_{81}		q_{100}	
A^{11}	λ_5		q_{15}		q_{34}		q_{53}		q_{72}		q_{91}		q_{110}

Truncated Contributions to Multi-Wave Roll Model

$$\mathbf{q} = [u, v, w, T]^T$$

To 1st Nonlinear Landau Term:

$0 + A^2 q_{01}$	(mean flow modification)
$Aq_{10} + 0 + A^3 q_{11}$	(fundamental wavelength)
$0 + A^2 q_{20}$	(1st harmonic)
$0 + 0 + A^3 q_{30}$	(2nd harmonic)

Low-Order Truncation Errors

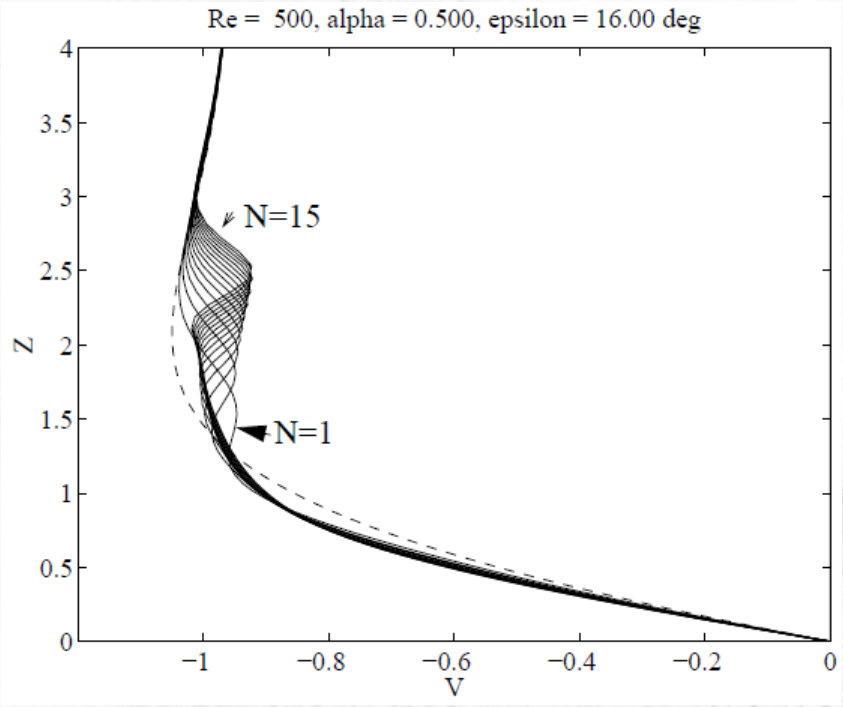

Mean-flow Modification

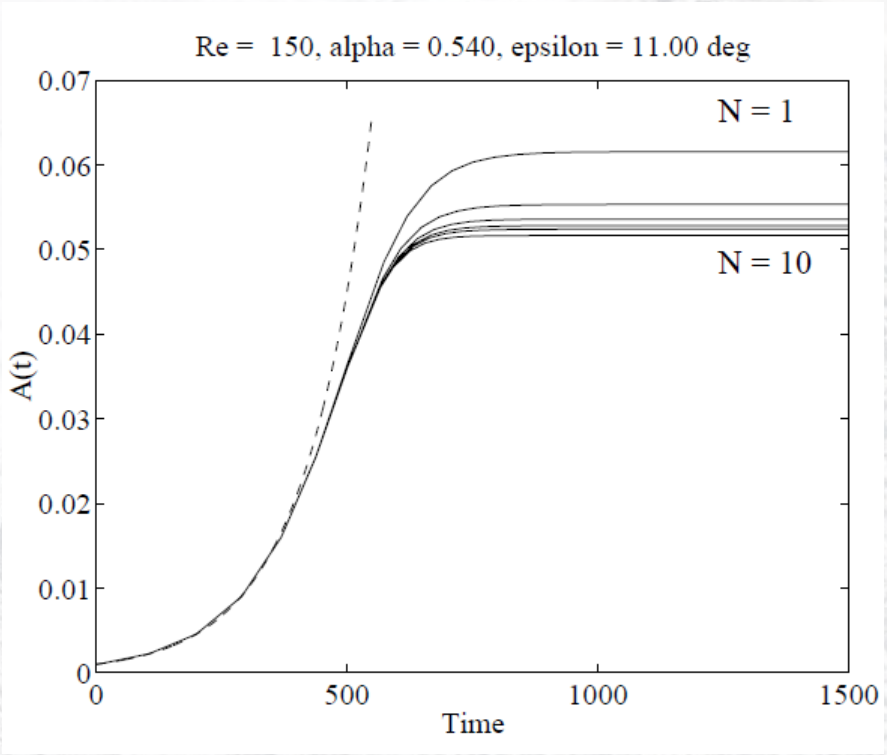

Amplitude Estimation

Upscale Transfer Resonant Triad

- $\alpha = \beta + \gamma$ (mode A, mode B, mode C)
- My nonlinear solution method restricts me[1] to all unstable modes
- Require at least one wavenumber at fastest growing mode
- For upscale transfer (into small wavenumber), intermediate wavenumber is usually also fast-growing

[1]but not necessarily reality

Truncated 3-Mode Roll Solutions

$$q_\alpha = Aq_{0,\alpha} + BCq_{1,\alpha}e^{i\phi} + A[A^2q_{2,\alpha} + B^2q_{3,\alpha} + C^2q_{4,\alpha}] + A^2q_{20,\alpha} + A^3q_{30,\alpha}$$

$$q_\beta = Bq_{0,\beta} + ACq_{1,\beta}e^{-i\phi} + B[A^2q_{2,\beta} + B^2q_{3,\beta} + C^2q_{4,\beta}] + B^2q_{20,\beta} + B^3q_{30,\beta}$$

$$q_\gamma = Cq_{0,\gamma} + ABq_{1,\gamma}e^{-i\phi} + C[A^2q_{2,\gamma} + B^2q_{3,\gamma} + C^2q_{4,\gamma}] + C^2q_{20,\gamma} + C^3q_{30,\gamma}$$

$$\phi = \theta_A - \theta_B - \theta_C$$

- **YELLOW**: contributions from single-wave theory; e.g. $q_{2,\alpha} = q_{11,\alpha}$, generates Landau coefficient.
- **BLUE**: new wave-wave & wave-mean flow interaction contributions. Each of these generates a new Landau coefficient.
- **RED:** Low-order phase-coupling wave-wave transfer terms.
- Also: mean-flow modifications due to each wave.

Truncated 3-Mode Model
Amplitude (real) and Phase (imaginary)

- $\frac{1}{A}\frac{dA}{dt} - i\frac{d\theta_A}{dt} = a_0 + a_1\frac{BC}{A}e^{i\phi} + [a_2A^2 + a_3B^2 + a_4C^2]$
- $\frac{1}{B}\frac{dB}{dt} - i\frac{d\theta_B}{dt} = b_0 + b_1\frac{AC}{B}e^{-i\phi} + [b_2A^2 + b_3B^2 + b_4C^2]$
- $\frac{1}{C}\frac{dC}{dt} - i\frac{d\theta_C}{dt} = c_0 + c_1\frac{AB}{C}e^{-i\phi} + [c_2A^2 + c_3B^2 + c_4C^2]$
- $\phi = \theta_A - \theta_B - \theta_C$ (Wave phase imbalance)
- $\alpha = \beta + \gamma$ (resonant triad wavenumbers)

- The a_i, b_i, c_i are Landau coefficients, calculated via an orthogonalization assumption (nonlinear wave-wave & wave-mean flow interactions)
- Highest-order (bracketed) terms force equilibrium; dominated by single-wave contributions (a_2A^2, b_3B^2, c_4C^2)
- Lower-order phase coupling allows inter-scale energy transfer, ENHANCES GROWTH RATE OF SLOWEST-GROWING MODE, ESPECIALLY DURING QUASI-LINEAR PHASE

Quasi-Linear Approximation

- $\frac{d\phi}{dt} = \Delta\omega - [\ |a_1|\ \frac{BC}{A}\ \sin(\phi + \phi_{a1}) +$
  $|b_1|\ \frac{AC}{B}\ \sin(\phi - \phi_{b1}) +$
  $|c_1|\ \frac{AB}{C}\ \sin(\phi - \phi_{c1})\ ]$
- $\frac{dA}{dt} = a_0 A + |a_1|\ BC \cos(\phi + \phi_{a1})$
- $\frac{dB}{dt} = b_0 B + |b_1|\ AC \cos(\phi - \phi_{b1})$
- $\frac{dC}{dt} = c_0 C + |c_1|\ AB \cos(\phi - \phi_{c1})$
- $a_1 = |a_1| \exp(\phi_{a1})$, & etc.
- $\Delta\omega = \omega_\alpha - \omega_\beta - \omega_\gamma$
- $\lambda_\alpha = a_0 + i\,\omega_\alpha$ (& etc., eigenvalues)

A,B grow faster than C:
$\therefore$ This term dominates $\frac{d\phi}{dt}$

Enhanced growth of C if:
$\phi - \phi_{c1} \sim 2n\pi$

Quasi-Linear Approximation (cntd.)

- A & B initially grow faster than C
- $\frac{d\phi}{dt} \sim |c_1| \frac{A_0 B_0}{C_0} \exp[(a_0+b_0-c_0)t] \sin(\phi - \phi_{c1})$
  - Net effect: $\phi - \phi_{c1} \rightarrow 2n\pi$
- $\frac{dC}{dt} \dashrightarrow c_0 C + |c_1| AB$
  - Accelerates growth of mode C

Phase-Coupling: Energizing Slowest-Growing Mode

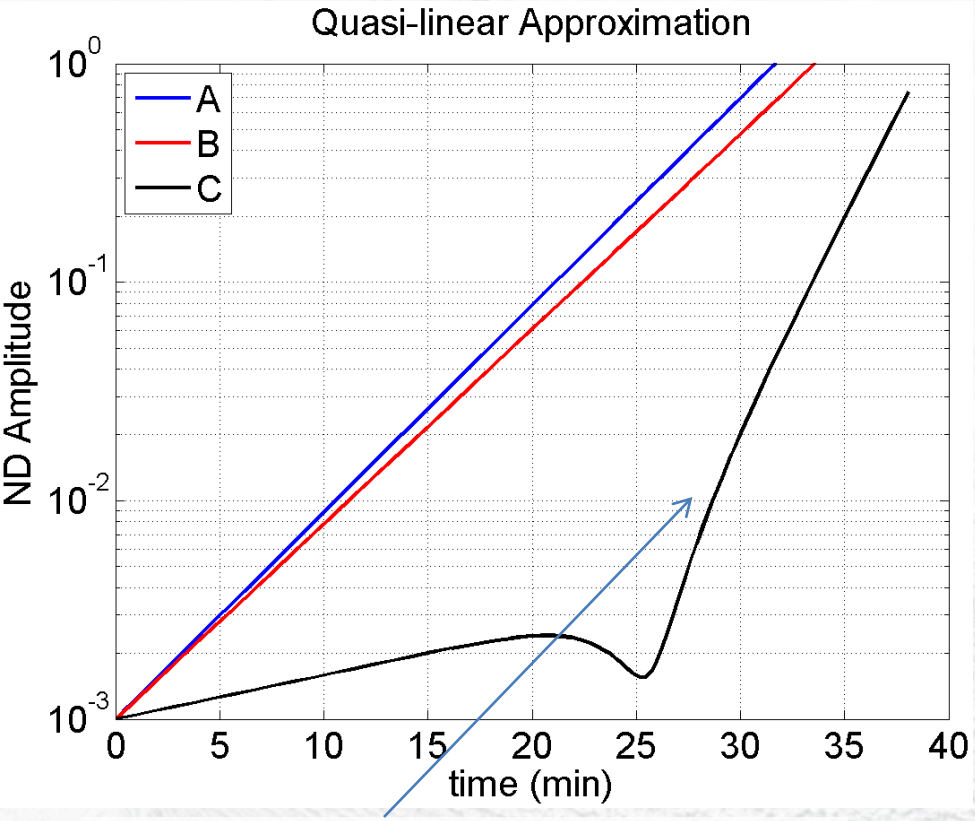

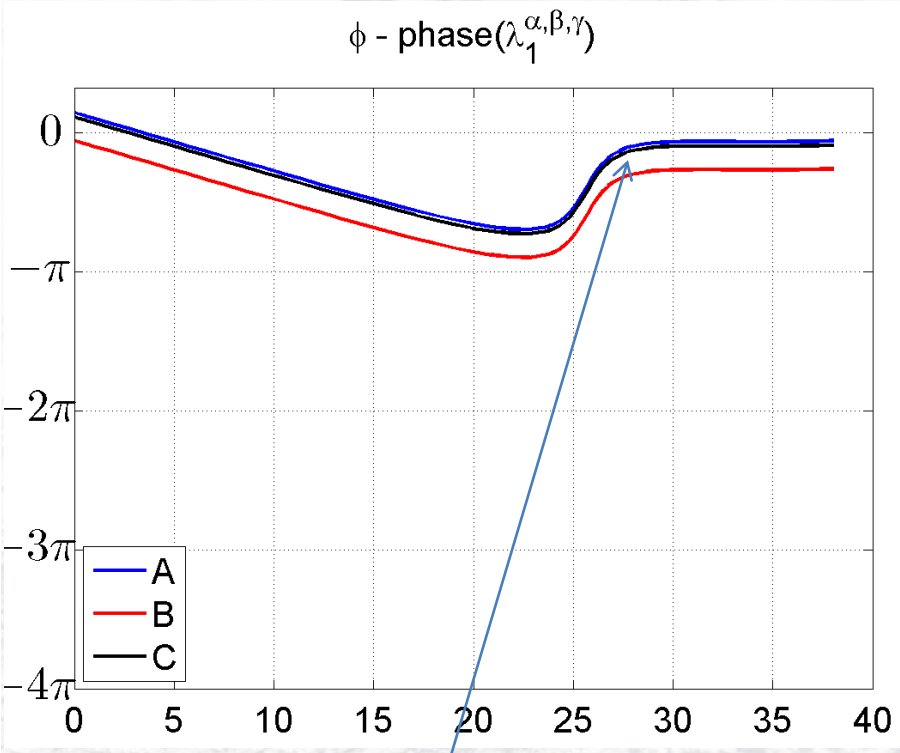

Accelerated growth of slow mode (C)

$\phi = \theta_A - \theta_B + \theta_C$
Phase Imbalance

Starts when ($\phi - \phi_{c1}$) → $2\pi n$
This must happen due to phase coupling.

TC PBL Mean Flow from Foster (2009)

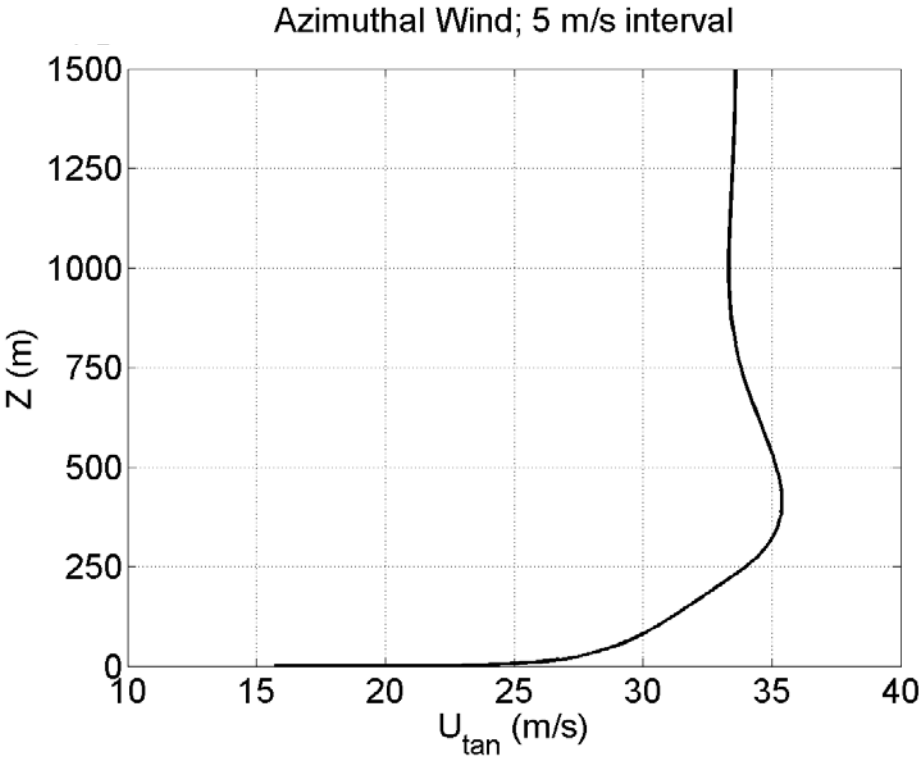

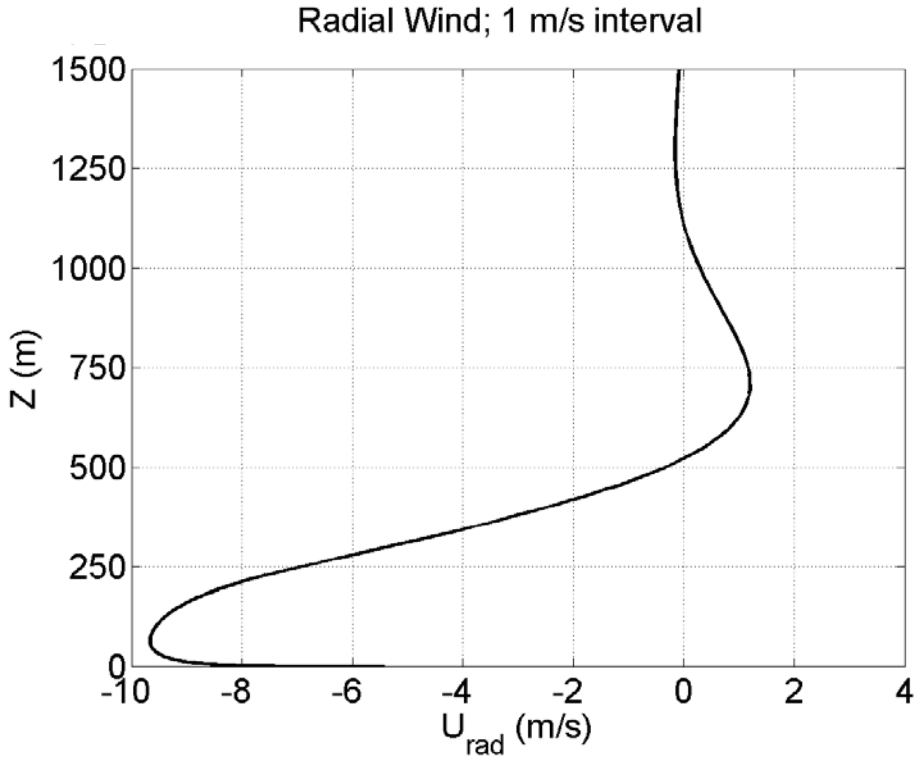

GROWTH RATE CONTOURS VS. WAVENUMBER AND ORIENTATION ANGLE

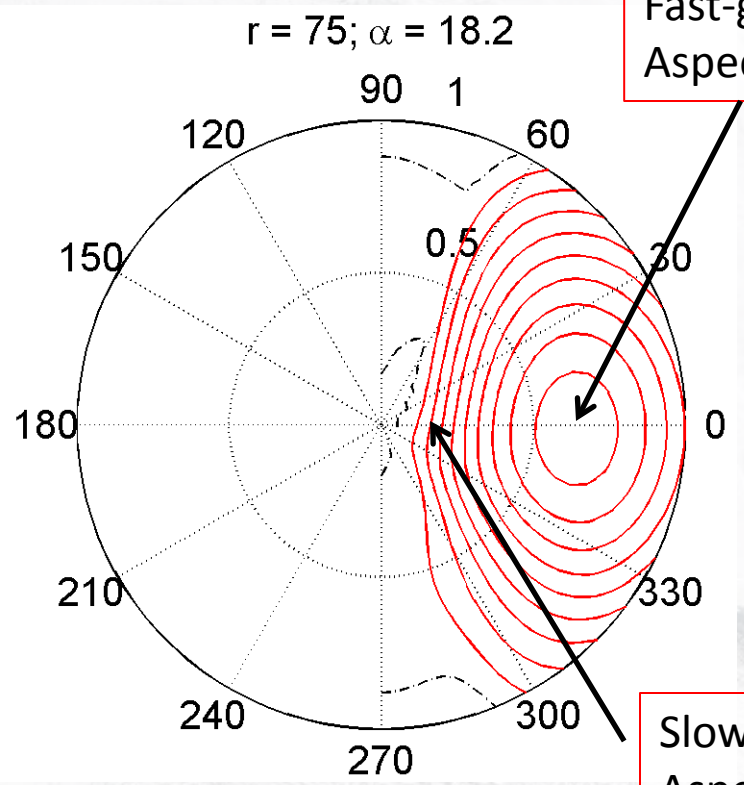

Fast-growing, *O*(2.5)
Aspect Ratio Modes

Slow-growing, *O*(10)
Aspect Ratio Modes

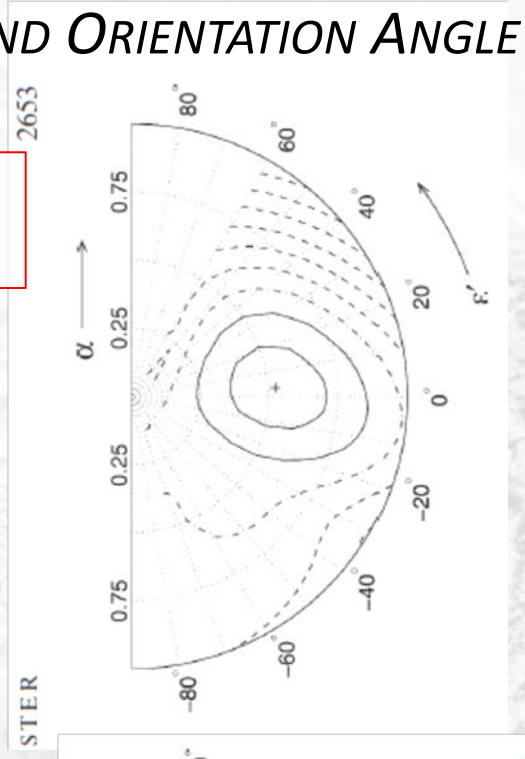

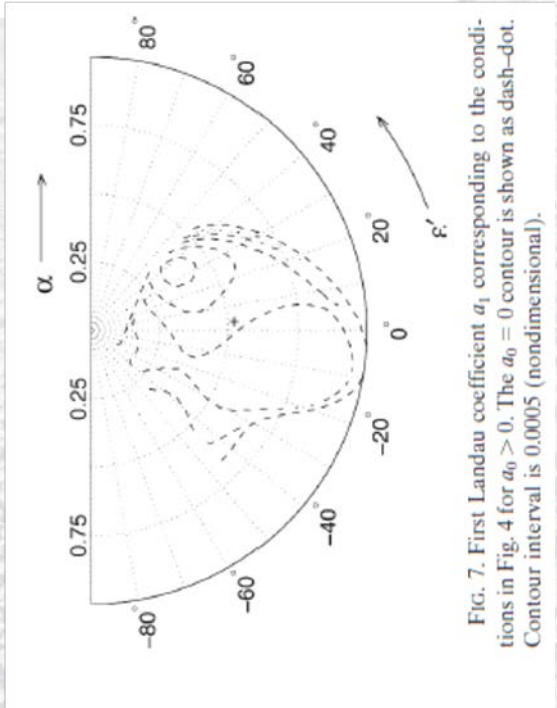

FIG. 7. First Landau coefficient a_1 corresponding to the conditions in Fig. 4 for $a_0 > 0$. The $a_0 = 0$ contour is shown as dash–dot. Contour interval is 0.0005 (nondimensional).

Dominant modes match observations
~sub-km to 2 to 3 km wavelengths

Large aspect ratio modes are too slowly-growing
To compete with lower aspect ratio modes

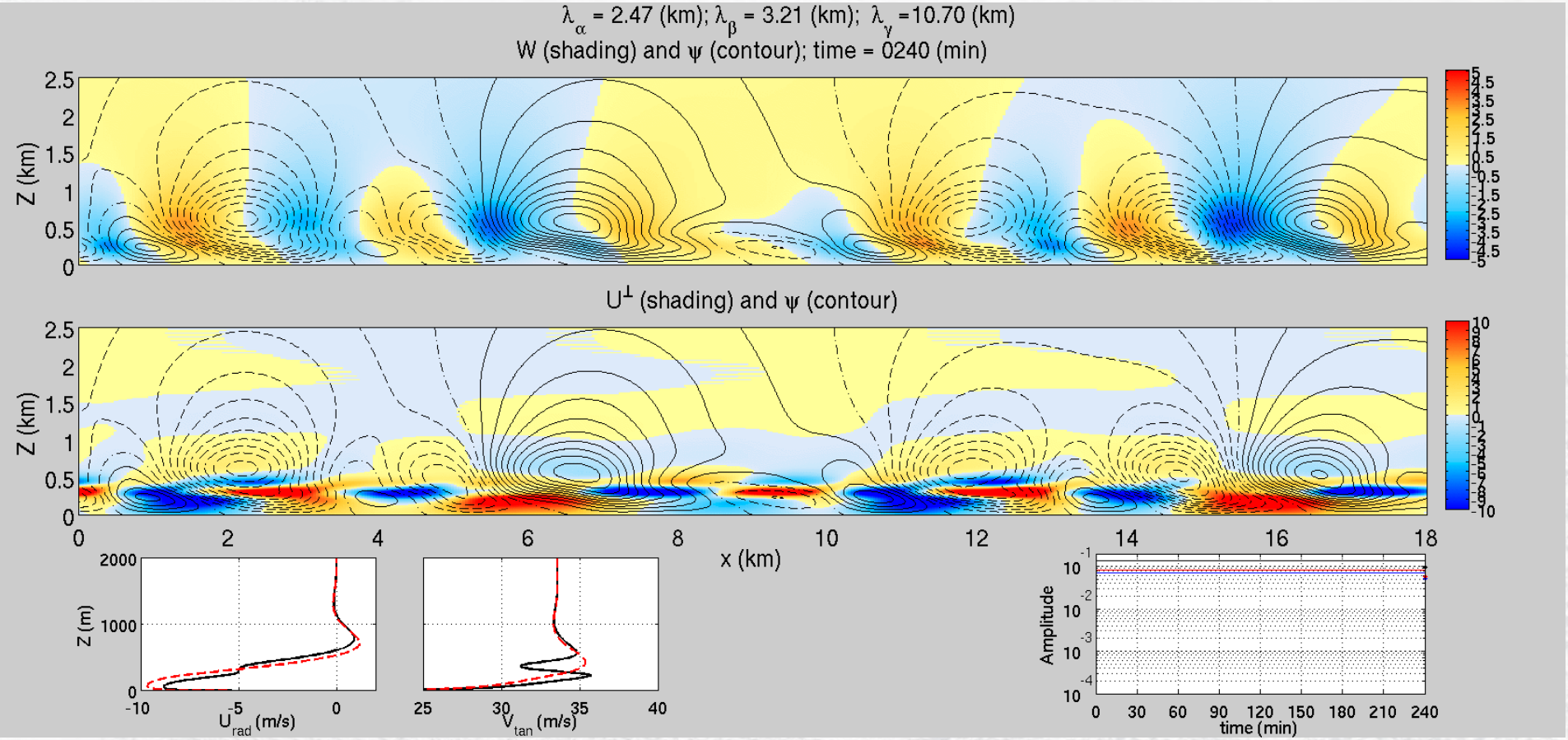

Contours are Overturning Flow Streamfunction (ψ)

Colors are: top, vertical velocity (W) (top); bottom, along-roll ($U^{\perp}$)

Note: Large aspect ratio modes extends above the PBL

Any Other Evidence?

Small-Scale Spiral Bands Observed in Hurricanes Andrew, Hugo, and Erin

MWR, **126**, 1998

ROBERT GALL, JOHN TUTTLE, AND PETER HILDEBRAND

National Center for Atmospheric Research, Boulder, Colorado

(Manuscript received 7 July 1997, in final form 10 October 1997)

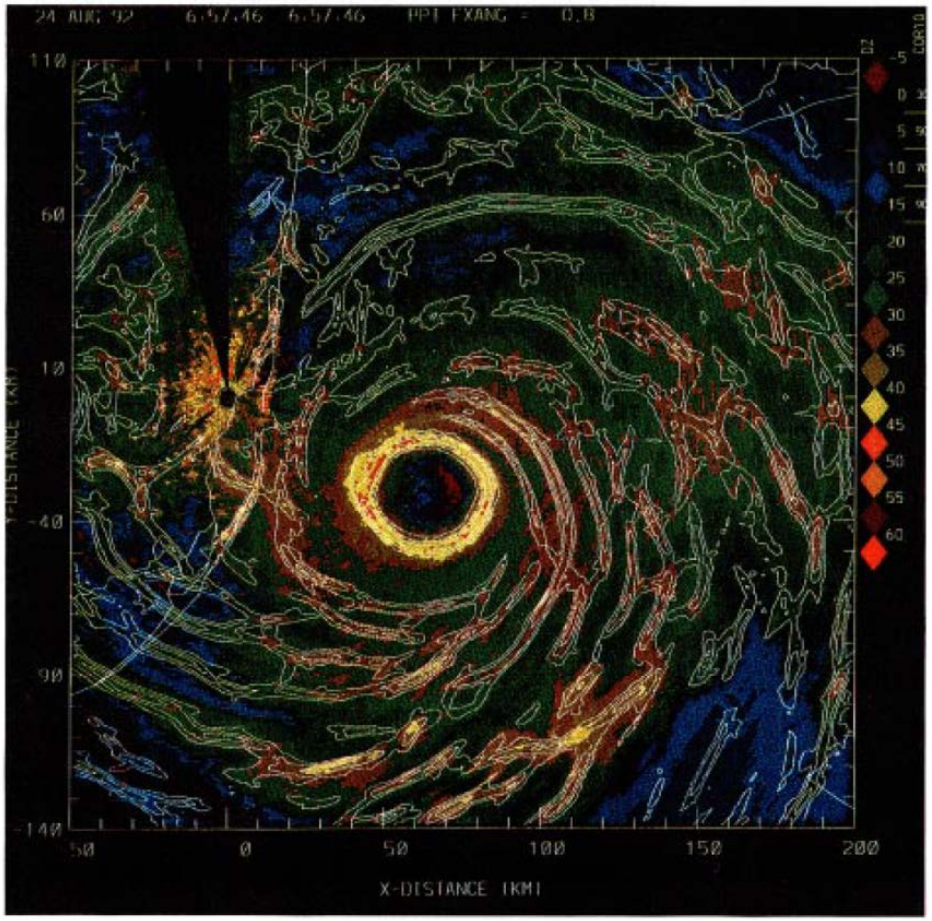

FIG. 5. Correlation field from the correlation analysis of the Andrew data from Fig. 1, using $\lambda = 10$, white contours, superimposed on the Fig. 1 radar reflectivity field. Contours start at 0.3 and increment by 0.1. Reflectivity scale same as Fig. 1.

5. Conclusions

The above analysis provides clear evidence for the existence of relatively small-scale (~10 km) spiral features of rather deep vertical extent near the eyes of three hurricanes. We suspect that these small-scale spiral features are present in most intense hurricanes. Using the radar and in situ data, we have been able to describe many features of these small-scale spiral bands, but the question remains, what are they? At this point we can only offer suggestions, since a definitive description of their structure is not available from the data at hand.

We know that the small-scale bands are on the order of 5 km deep and have spatial scales on the order of 10 km. The higher-reflectivity regions have stronger updrafts and greater equivalent potential temperature than do regions of lower reflectivity. These small-scale bands appear to line up approximately with the low-level wind, where the radial component of the flow is part of the total wind. They move approximately with the mean tangential wind throughout their depth. They exist near the center of the hurricane where the environment is saturated nearly everywhere and the lapse rates are neutral to moist ascent. It is our suggestion that these small-scale rainbands are similar to the rolls that exist in the planetary boundary layer and other flows, that are driven by the boundary layer shear in the presence of convection. Such rolls often have 1:2 aspect ratios, such as described here. We are confused by the depth of the these hurricane bands, however, since they are much deeper than we would have expected for classic boundary layer rolls. Perhaps the environment in the inner 100 km or so of the hurricane is unstable enough, wet enough, and contains enough liquid water (so that weak downdrafts associated with the band structure undergo moist adiabatic processes) and these properties hold through deep enough layers that deep structures typical of boundary layer rolls could develop. Definitive an-

Note: Their definition of aspect ratio is different

Zach Gruskin (grad student) and Prof. Greg Tripoli, Univ. Wisconsin (*pers. comm.*)

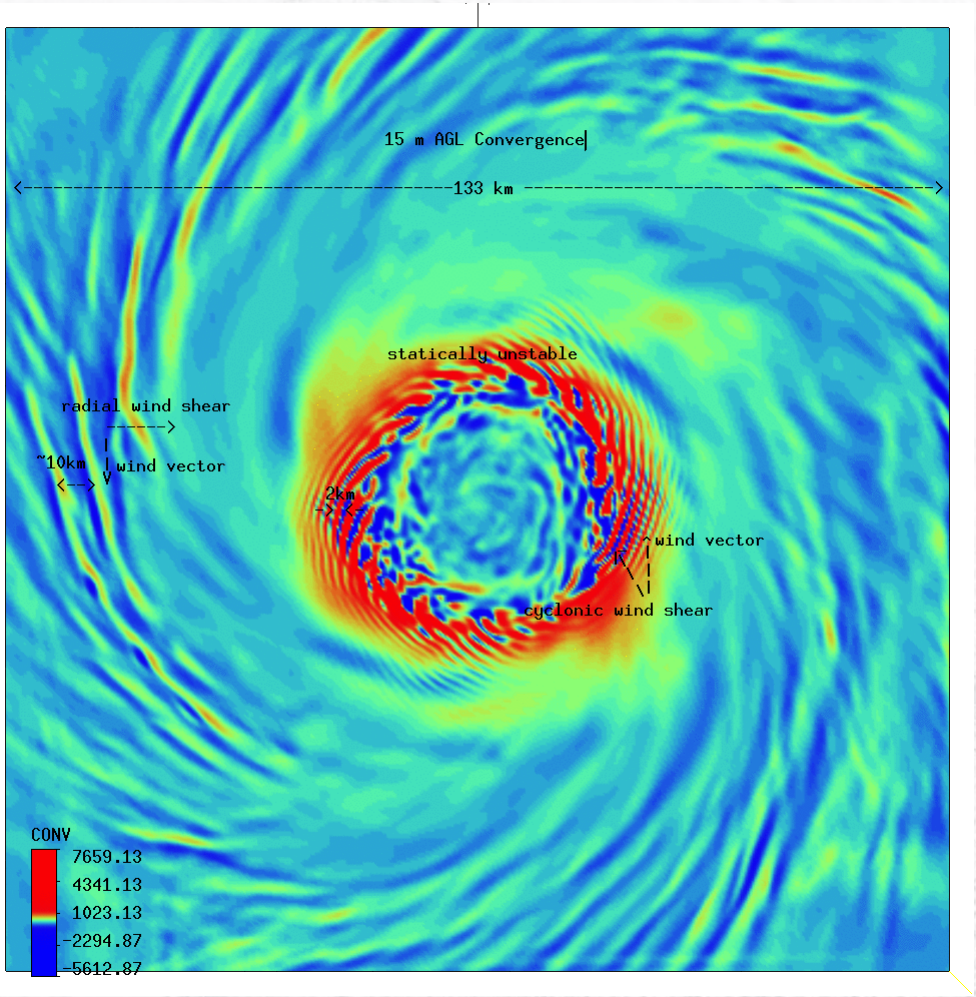

333 m resolution numerical model of TC flow

Consistent feature in the simulations

133 km box

15 m Divergence field

Motivation for Study

- Can this signal be used to improve SAR (or UHR scatterometer) surface wind retrievals?
  - Orientation relative to the surface wind, mean shear, mean PBL wind?
- Do the large rolls affect PBL fluxes?
- Do they affect air-sea interaction?
  - Wind stress curl?

Signature may be clearer in (ρ=const) WSC than in DIV

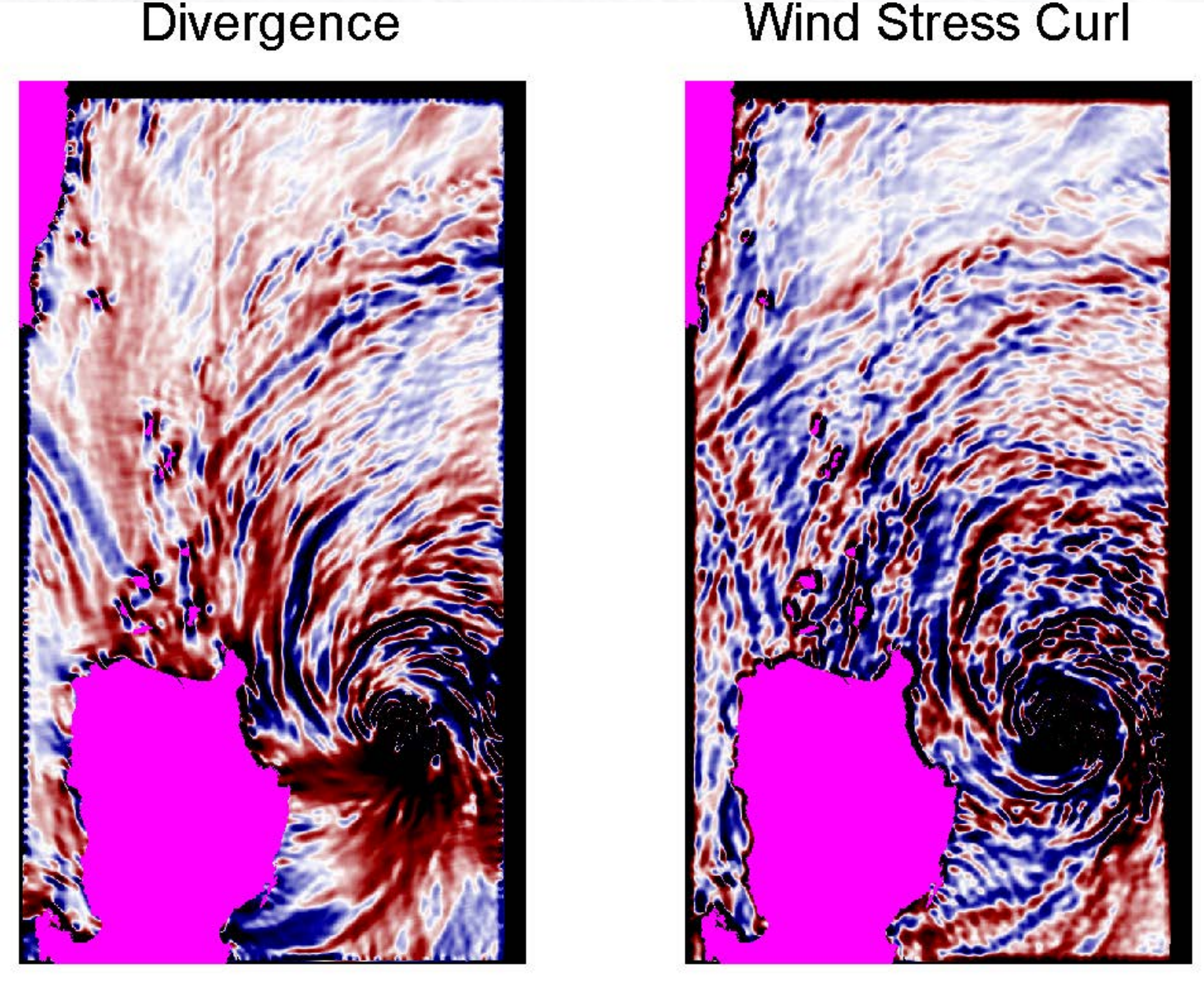

Summary

- **ALL SAR TC SCENES SHOW SURFACE WIND ORGANIZATION AT *O*(10 KM) WAVELENGTH; CONSISTENT WITH LARGE ASPECT RATIO PBL ROLLS**
  - 1 km SAR wind pixels (from 25 m σ_0 pixels); SLP-filtered winds
  - Consistent with Gall et al. (1998) radar data and brand-new Gruskin & Tripoli numerical modeling research
- **LOW-ORDER PHASE COUPLING IN WAVE-WAVE INTERACTION MODEL FEEDS ENERGY FROM THE DOMINANT ROLLS INTO THE SLOWLY-GROWING LONG-WAVELENGTH ROLLS**
  - TC PBLs nearly always form *O*(2 km) wavelength rolls
  - Simple and reasonable mechanism for large aspect ratio rolls
  - Mechanism remains to be proven by experiment
- Future work
  - Does this mechanism explain variability in detection of 2 km rolls in TCs?
  - Extend to non-co-linear waves (string of pearls)
  - Cold-air outbreaks
  - Resonant tetrads? (see extra slides)
  - Higher-order truncations

Extra Slides

Example:

J. Wurman, Doppler on Wheels, Hurricane Rita, 2005

- 1.2° slices every 12 seconds
- Radial Velocity
- Gate Spacing 25 m
- Azimuthal Resolution 0.25°
- 2 km Range Rings (8 km shown)

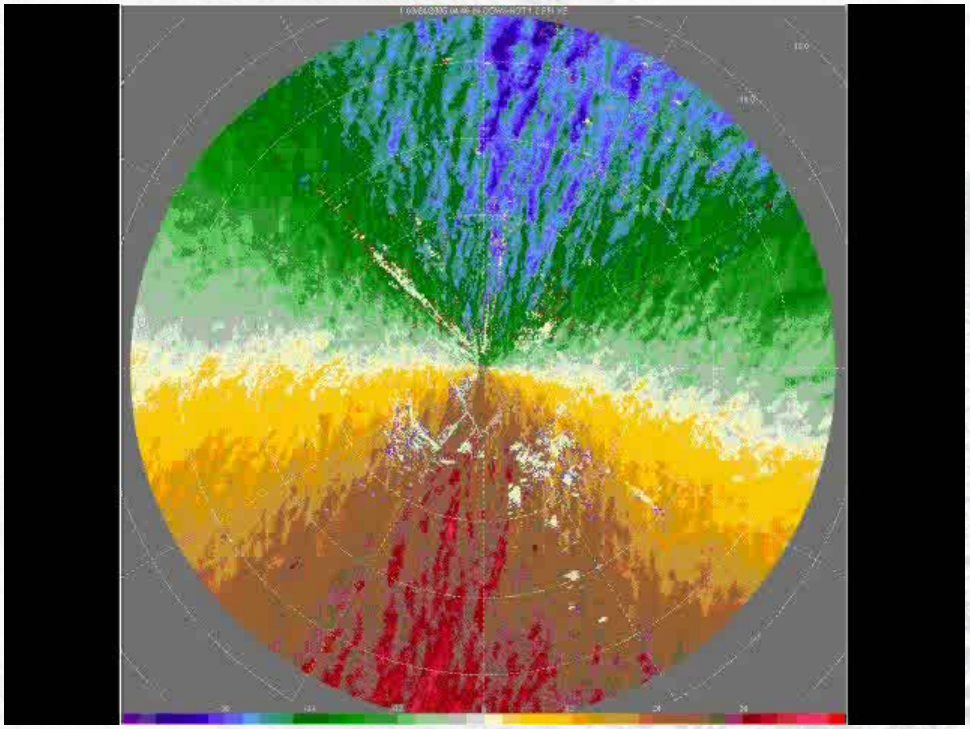

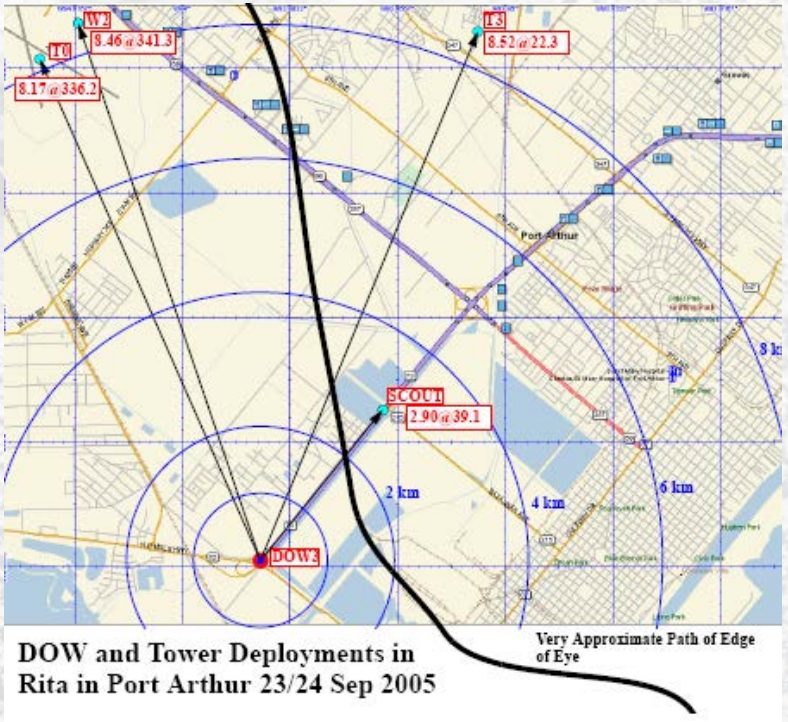

DOW and Tower Deployments in Rita in Port Arthur 23/24 Sep 2005

Very Approximate Path of Edge of Eye

dicular to the rolls.

Radar volumes were updated every 300 s; these intervals were too long to permit esti-

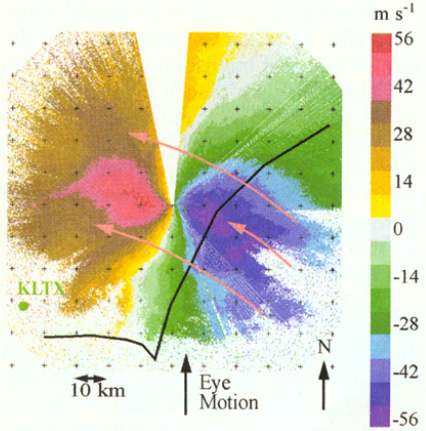

Fig. 3. Large-scale Doppler velocity structure at 23:30:19 UTC, as measured by the DOW radar. Strong easterly flow peaking at ~60 m s^{-1} is evident both off- and onshore. The eye of the hurricane is at the edge of radar visibility to the south. Visibility was severely limited by attenuation. Pink curved arrows illustrate average wind flow. Scan is at 5° elevation.

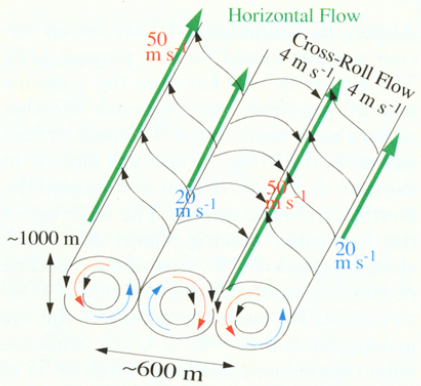

Fig. 5. Schematic representation of observed shear- and wind-parallel boundary layer rolls. High-momentum air (red) is brought to the surface in the downward legs of the rolls, while air slowed near the surface is brought aloft in the upward legs.

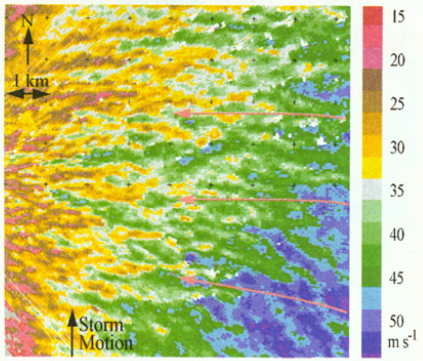

Fig. 4. High-resolution image of Doppler velocity field to the east of Wilmington at 23:58:17 UTC. Sub-kilometer-scale streaks caused by boundary layer rolls modulate the mean easterly flow. Near the radar (left) at altitudes of ~100 m agl, peak and trough wind speed values are ~40 m s^{-1} and ~10 m s^{-1}, respectively. Further from the radar (right), peak and trough wind speed values alternate from ~25 to ~55 m s^{-1}. Azimuthal shear values are (~30 m s^{-1}/~300 m) ≈ 0.1 s^{-1} across many of the rolls. Scan is at 2° elevation.

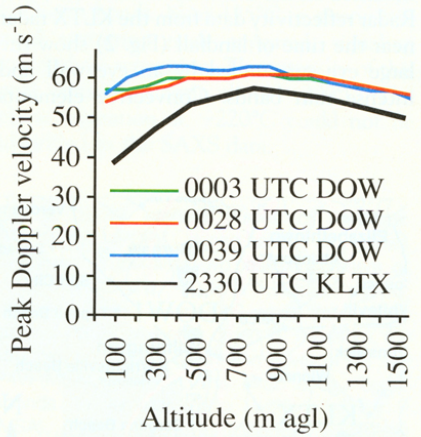

Fig. 6. Altitude dependence of peak wind speeds as observed by DOW and National Weather Service KLTX radars. DOW-measured peak speeds at 100 m agl are nearly as high as those at 1000 m agl as a result of momentum transport in the rolls and agree closely with surface peak wind observations. KLTX-measured peak speeds are smaller at low altitude because of poorer resolution and possibly because of longer overland trajectories.

~30 m/s mean +/- 15 m/s across-roll variation in low-level wind

Wurman and Winslow (1998) *Science*, **280,** 555-557

Transfer Moderate (~3 km) to Small (sub-km) Scales

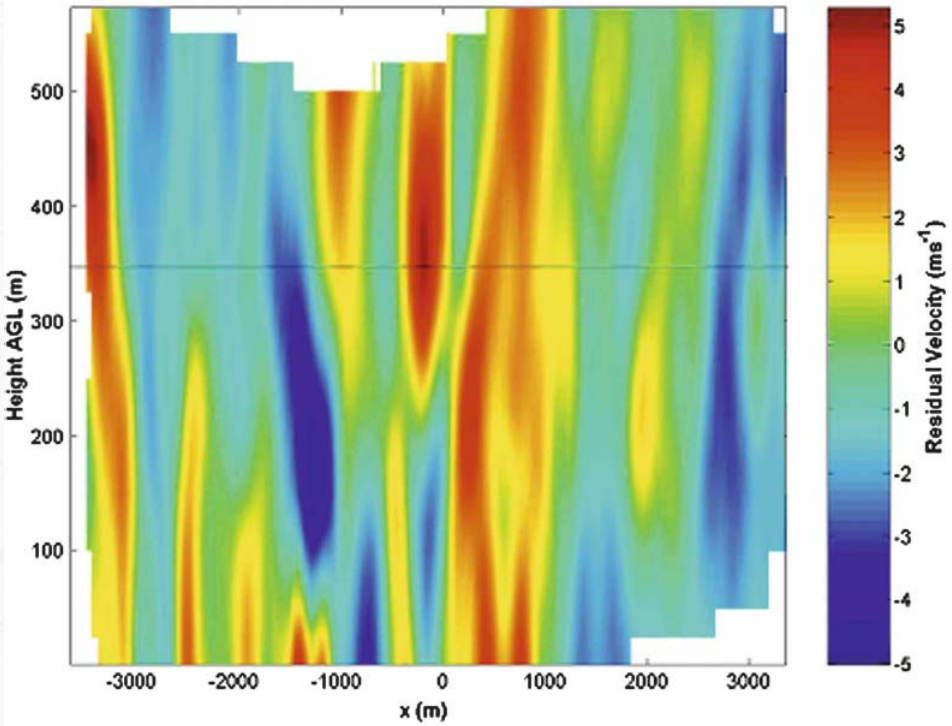

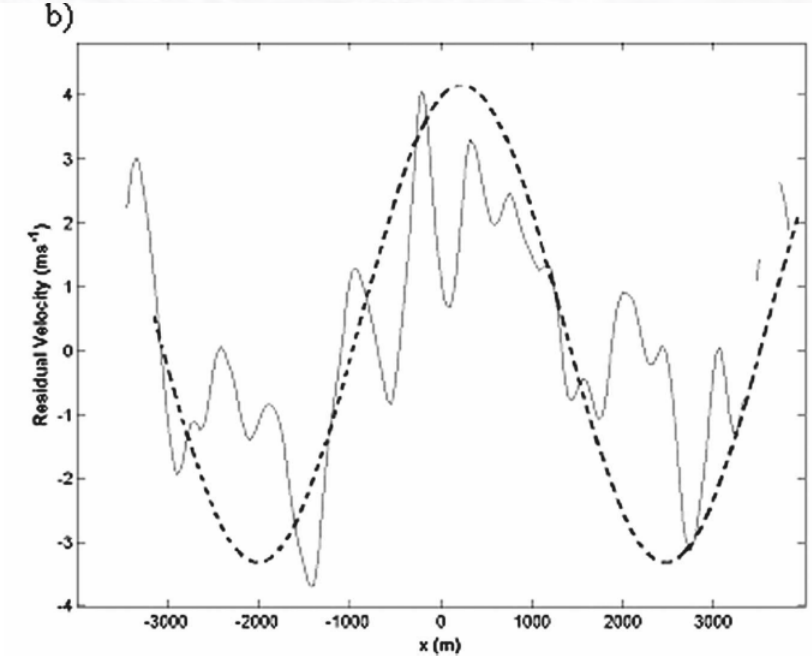

FIG. 16. Example of superposition of scales of motion. (a) Vertical cross section of residual radial velocity from Hurricane Frances. The solid line indicates the height at which the data presented in (b) were extracted. (b) The thin line represents the individual residual velocity data at 350 m AGL, and the dashed line outlines the larger scales of motion superimposed on the signal.

An Observational Study of Hurricane Boundary Layer Small-Scale Coherent Structures

SYLVIE LORSOLO AND JOHN L. SCHROEDER

Atmospheric Science Group, Texas Tech University, Lubbock, Texas

PETER DODGE AND FRANK MARKS JR.

Hurricane Research Division, NOAA Atlantic Oceanographic and Meteorological Laboratory, Miami, Florida

(Manuscript received 4 June 2007, in final form 7 January 2008)

ABSTRACT

An Observational Case for the Prevalence of Roll Vortices in the Hurricane Boundary Layer*

IAN MORRISON AND STEVEN BUSINGER
University of Hawaii at Manoa, Honolulu, Hawaii

FRANK MARKS AND PETER DODGE
Hurricane Research Division, NOAA/AOML, Miami, Florida

JOOST A. BUSINGER
University of Washington, Seattle, Washington

(Manuscript received 5 April 2004, in final form 12 December 2004)

Boundary-Layer Meteorol (2008) 128:173–189
DOI 10.1007/s10546-008-9281-2

ORIGINAL PAPER

Effects of Roll Vortices on Turbulent Fluxes in the Hurricane Boundary Layer

Jun A. Zhang · Kristina B. Katsaros · Peter G. Black · Susanne Lehner · Jeffrey R. French · William M. Drennan

VOLUME 62 JOURNAL OF THE ATMOSPHERIC SCIENCES AUGUST 2005

Why Rolls are Prevalent in the Hurricane Boundary Layer

RALPH C. FOSTER
Applied Physics Laboratory, University of Washington, Seattle, Washington

(Manuscript received 5 April 2004, in final form 1 December 2004)

ABSTRACT

JOURNAL OF GEOPHYSICAL RESEARCH, VOL. 113, D17104, 16 PP., 2008
doi:10.1029/2007JD009643

Simulation and parameterization of the turbulent transport in the hurricane boundary layer by large eddies

Ping Zhu
Department of Earth Sciences, Florida International University, Miami, Florida, USA

AUGUST 2008 LORSOLO ET AL. 2871

An Observational Study of Hurricane Boundary Layer Small-Scale Coherent Structures

SYLVIE LORSOLO AND JOHN L. SCHROEDER
Atmospheric Science Group, Texas Tech University, Lubbock, Texas

PETER DODGE AND FRANK MARKS JR.
Hurricane Research Division, NOAA Atlantic Oceanographic and Meteorological Laboratory, Miami, Florida

(Manuscript received 4 June 2007, in final form 7 January 2008)

ABSTRACT

JOURNAL OF GEOPHYSICAL RESEARCH, VOL. 115, D06205, 13 PP., 2010
doi:10.1029/2009JD011819

Helical circulations in the typhoon boundary layer

Ryan Ellis
Department of Meteorology, University of Hawai'i at Mānoa, Honolulu, Hawaii, USA

Steven Businger
Department of Meteorology, University of Hawai'i at Mānoa, Honolulu, Hawaii, USA

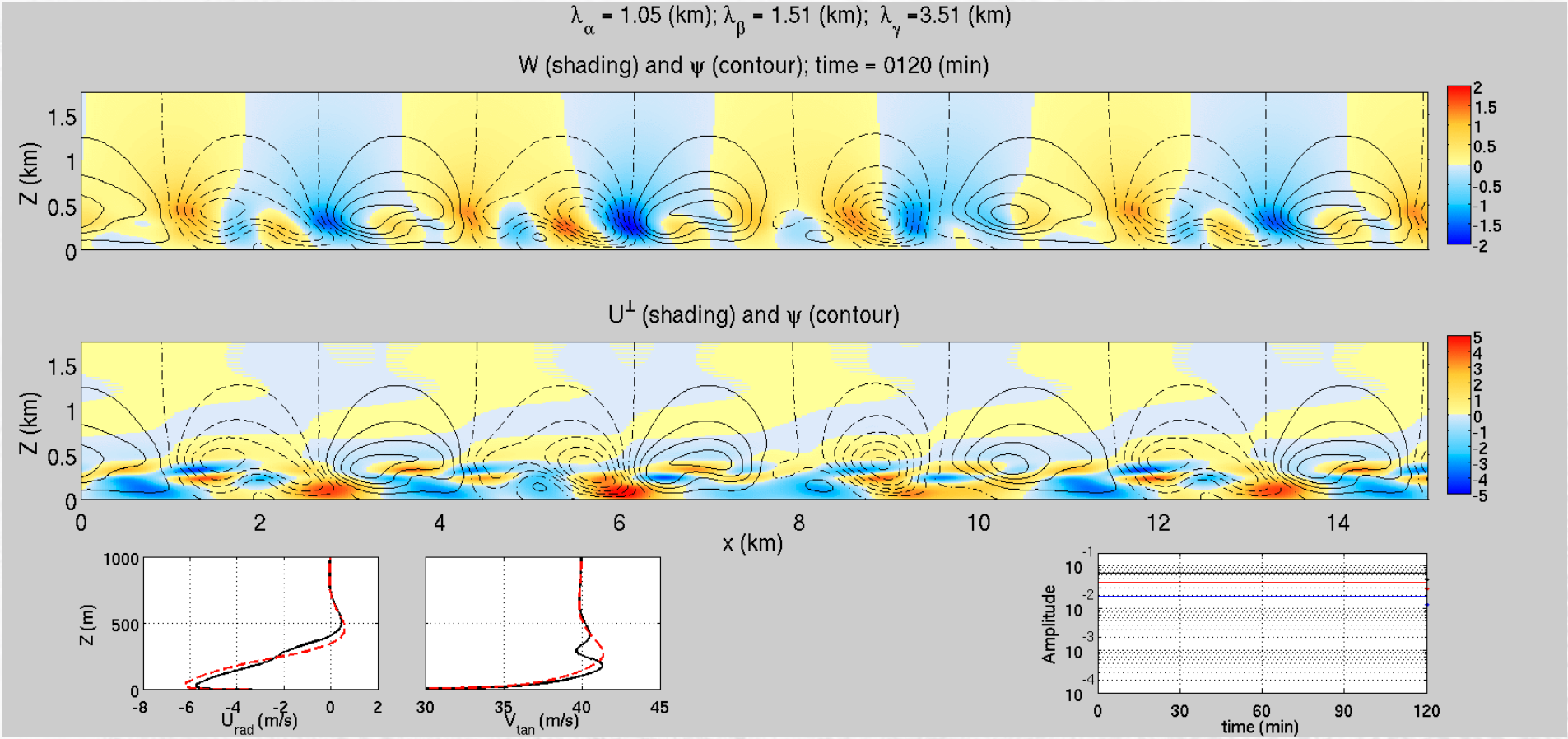
λα = 1.05 (km); λβ = 1.51 (km); λγ =3.51 (km)
W (shading) and ψ (contour); time = 0120 (min)
Z (km)
U⊥ (shading) and ψ (contour)
x (km)
Z (m)
Urad (m/s)
Vtan (m/s)
Amplitude
time (min)

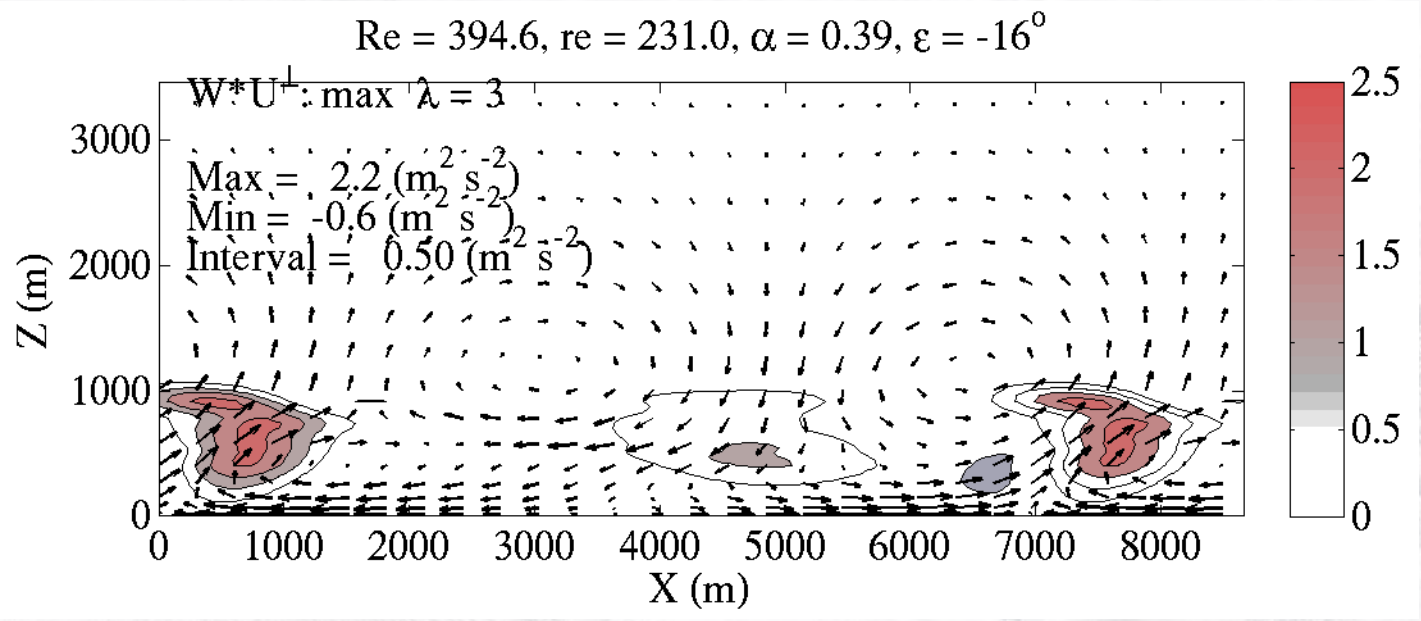

Non-local
vw (~along)

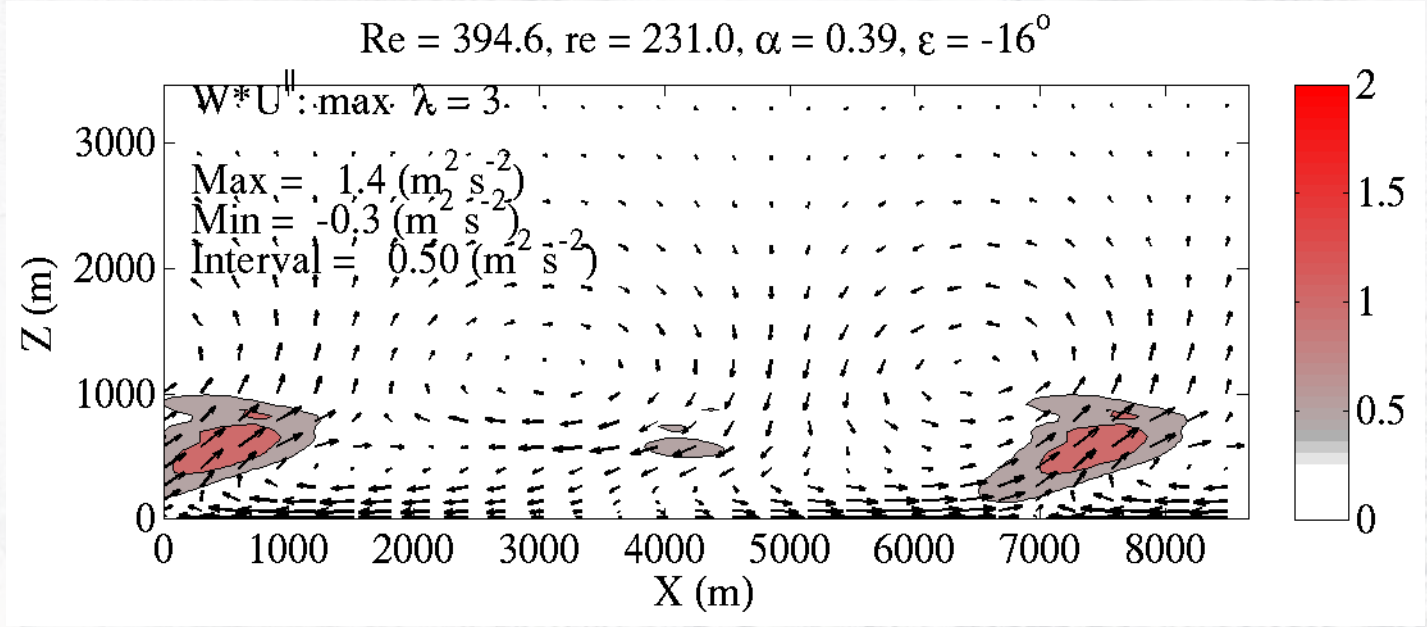

Non-local
uw (~across)

Wavelength: ~ 6km; orientation : – 16°

How do rolls fit into overall TCBL momentum balance?

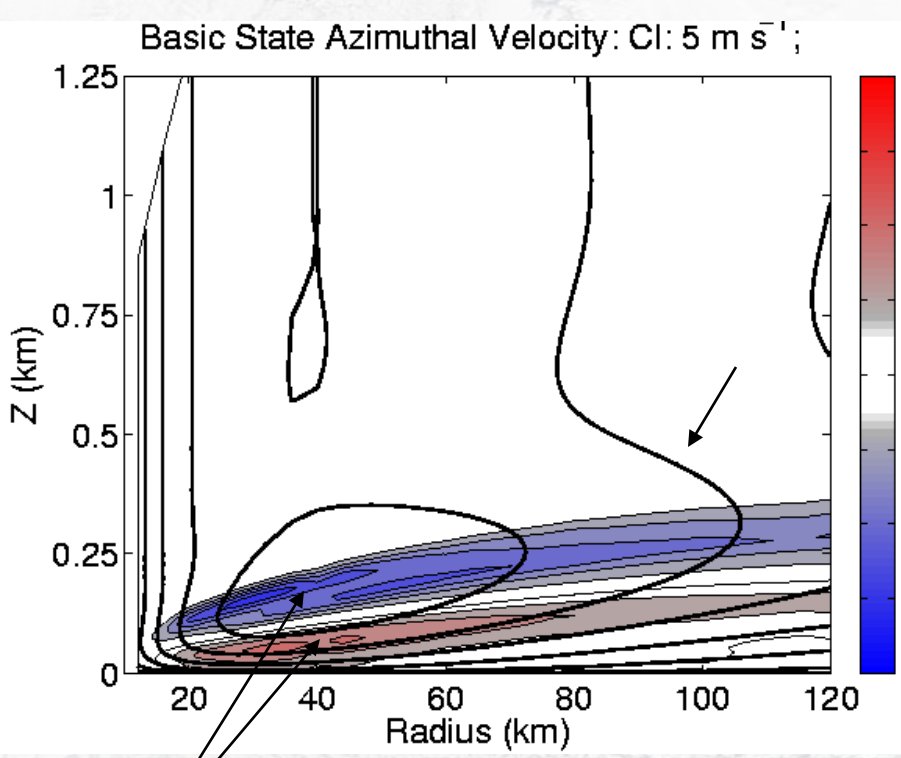

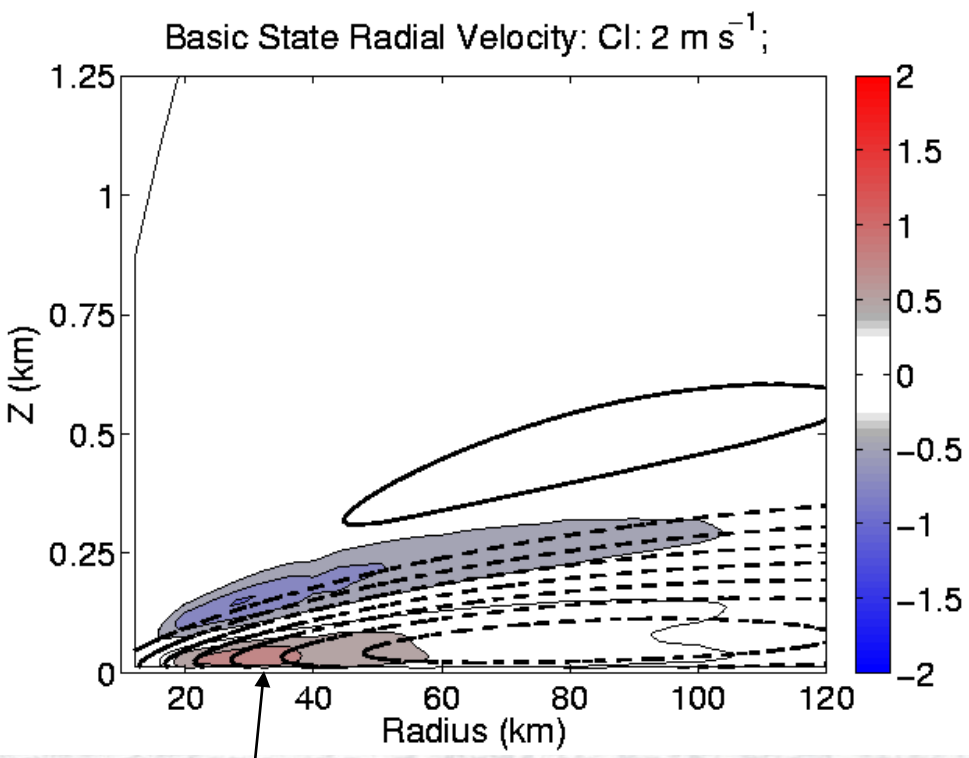

Rolls nonlocally transfer Super-Gradient Jet momentum towards surface

Weakened near-surface inflow near and inside RMW